Available online at www.sciencedirect.com
SCIENCE DIRECT®
ELSEVIER
Journal of Nuclear Materials 320 (2003) 177–183
journal of nuclear materials
www.elsevier.com/locate/jnucmat

Atom probe tomography characterization of radiation-sensitive KS-01 weld

M.K. Miller [a,*], K.F. Russell [a], M.A. Sokolov [b], R.K. Nanstad [b]

[a] *Microscopy, Microanalysis, Microstructures Group, Metals and Ceramics Division, Oak Ridge National Laboratory, P.O. Box 2008 Building 4500S, Oak Ridge, TN 37831-6136, USA*

[b] *Radiation Materials Science and Technology Group, Metals and Ceramics Division, Oak Ridge National Laboratory, P.O. Box 2008 Building 4500S, Oak Ridge, TN 37831-6151, USA*

Received 4 November 2002; accepted 10 February 2003

Abstract

The microstructure of a radiation-sensitive KS-01 test weld has been characterized by atom probe tomography. The levels of copper, manganese, nickel and chromium in this weld were amongst the highest of all the steels used in Western reactor pressure vessels. After neutron irradiation to a fluence of 0.8×10^{23} n m^{-2} ($E > 1$ MeV) at a temperature of 288 °C, this weld exhibited a large Charpy T_{41J} shift of 169 K, a large shift of the fracture toughness transition temperature of 160 K, a decrease in upper shelf energy from 118 to ~78 J, and an increase in the yield strength from 600 to 826 MPa. However, the mechanical properties data conformed to the master curve. Atom probe tomography revealed a high number density (~3×10^{24} m^{-3}) of Cu-, Mn-, Ni-, Si- and P-enriched precipitates and a lower number density (~1×10^{23} m^{-3}) of P clusters.

PACS: 61.82.Bg; 62.20.Mk; 81.40.−z

1. Introduction

The microstructure of a neutron irradiated KS-01 weld has been characterized by atom probe tomography. This technique has been demonstrated to be an effective tool for the characterization of the microstructure of neutron irradiated pressure vessel steels due to the small size of the microstructural features that are produced during irradiation [1,2]. Atom probe tomography has been applied to many different types of Western and Russian reactor pressure vessel steels [3–15]. The results of these characterizations have been reviewed recently [3–6].

The atypical KS-01 test weld is being examined by the Heavy Section Steel Irradiation program at Oak Ridge National Laboratory to investigate the shape of the fracture–toughness master curve for highly embrittled pressure vessel steels. This weld was selected for characterization because its levels of copper, manganese, nickel and chromium were amongst the highest of all the steels used for the pressure vessels in Western nuclear reactors. Therefore, the response of this weld to neutron irradiation should provide important information on the effects of high copper, manganese, nickel and chromium levels on the mechanical properties and microstructure. This weld exhibited a high sensitivity to neutron irradiation at a relatively low fluence.

The focus of this study is to compare the mechanical properties and the microstructure of this weld to those of other pressure vessel steels and model alloys.

2. Experimental

The composition of this KS-01 test weld was Fe- 0.37 wt% Cu, 1.23% Ni, 1.64% Mn, 0.70% Mo, 0.47% Cr,

* Corresponding author. Tel.: +1-865 574 4719; fax: +1-865 241 3650.
E-mail address: millermk@ornl.gov (M.K. Miller).

0022-3115/03/$ - see front matter © 2003 Elsevier B.V. All rights reserved.
doi:10.1016/S0022-3115(03)00108-9

0.18% Si, 0.017% P, 0.012% S and 0.06% C (Fe-0.33at.% Cu, 1.17% Ni, 1.67% Mn, 0.41% Mo, 0.50% Cr, 0.36% Si, 0.031% P, 0.021% S and 0.28% C). A comparison of the composition with other pressure vessel steels used in nuclear reactors is shown in Fig. 1. The copper, nickel, manganese and chromium levels in the KS-01 weld were all amongst the highest of all the steels used in Western reactor pressure vessels. In addition, the phosphorus level in the weld (0.031 at.% P) was significantly higher than other welds.

The weld was given a stress relief heat treatment of 46.5 h at 550 °C plus 8 h at 600 °C prior to neutron irradiation. The weld was examined after the stress relief treatment and after neutron irradiation to a relatively low fluence of 0.8×10^{23} n m^{-2} ($E > 1$ MeV) at a temperature of 288 °C in the re-useable facility of the University of Michigan Ford Nuclear Reactor.

The microstructure of the weld was characterized with the Oak Ridge National Laboratory's energy-compensated optical position-sensitive atom probe. The analyses were acquired with a specimen temperature of 50 K, a pulse fraction of 20% of the standing voltage and a pulse repetition rate of 1.5 kHz. All atom probe compositions quoted in this paper are given in atomic percent.

The matrix composition of the weld after the stress relief treatment, as measured by atom probe tomography, is given in Table 1. A small decrease in the

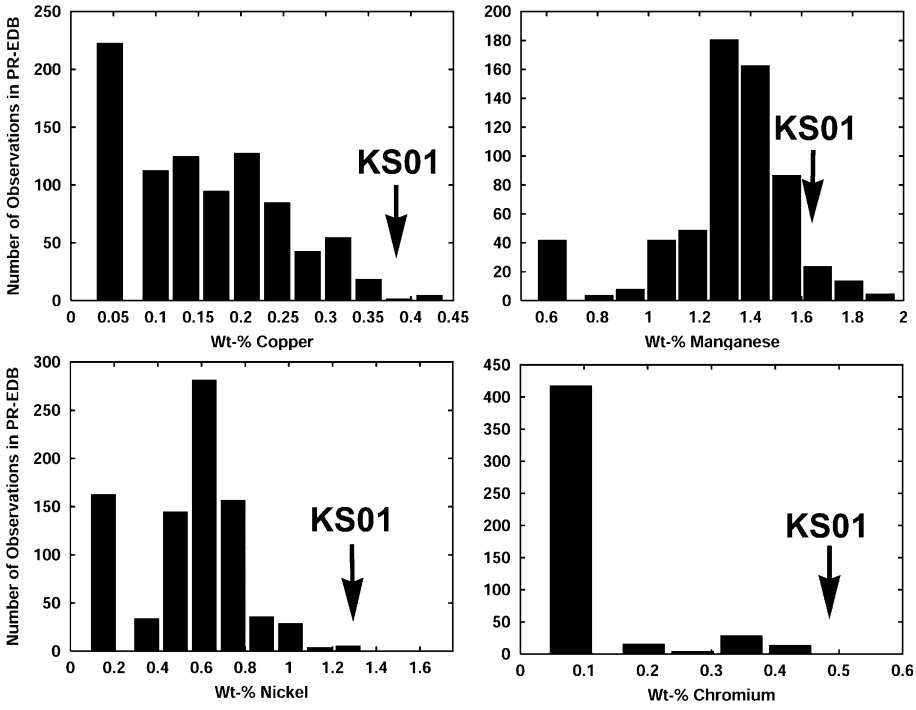

Fig. 1. Comparison of the composition of the KS-01 test weld with other pressure vessel steels in the PR-EDB database.

Table 1
Compositions of the ferrite matrix and the copper-enriched precipitates as estimated from atom probe data

Element	Alloy at.%	Unirradiated control	Ferrite matrix (no precipitates)	Copper-enriched precipitates
Cu	0.33	0.27 ± 0.01	0.16 ± 0.006	17.0 ± 9.7[a]
Ni	1.17	1.65 ± 0.01	1.16 ± 0.02	31.9 ± 13.8[a]
Mn	1.67	1.65 ± 0.02	1.17 ± 0.01	31.7 ± 11.8[a]
Mo	0.41	0.42 ± 0.01	0.28 ± 0.01	0.17 ± 0.17[a]
Cr	0.50	0.52 ± 0.01	0.55 ± 0.01	0.10 ± 0.10[a]
Si	0.36	0.36 ± 0.01	0.32 ± 0.01	1.7 ± 1.7[a]
P	0.031	0.02 ± 0.005	0.03 ± 0.005	0.20 ± 0.20[a]
C	0.28	0.10 ± 0.01	0.06 ± 0.005	0.01 ± 0.01[a]

All data is atomic percent.

[a] These standard deviations are based on the non-biased or '$n - 1$' method.

copper level from the nominal level of 0.33 to 0.27 at.% Cu was observed. A nitrogen level of $0.033 \pm 0.005\%$ N was measured in the matrix of the unirradiated control.

The presence of clusters was determined with the maximum separation method [1]. This method is based on the premise that the distance between solute atoms in a solute-enriched cluster or precipitate is significantly smaller than that in the surrounding matrix. Therefore, the atoms that belong to a solute-enriched cluster may be distinguished from those in the matrix based on a maximum separation distance, d_{max}. Computer simulations of random solid solutions with a body centered cubic crystal structure with the α-Fe lattice parameter ($a_0 = 0.288$ nm) and a detection efficiency of 60% were used to define the value of d_{max} and the minimum number of solute atoms associated with each cluster, n_{min}. Based on these simulations and the analysis of the data from the unirradiated material, parameters of $d_{max} = 0.5$ nm and $n_{min} = 10$ atoms were used for the analysis of the data from the neutron-irradiated weld to exclude fluctuations consistent with the random solid solution. The size of the solute-enriched features was estimated in terms of the radius of gyration, which was

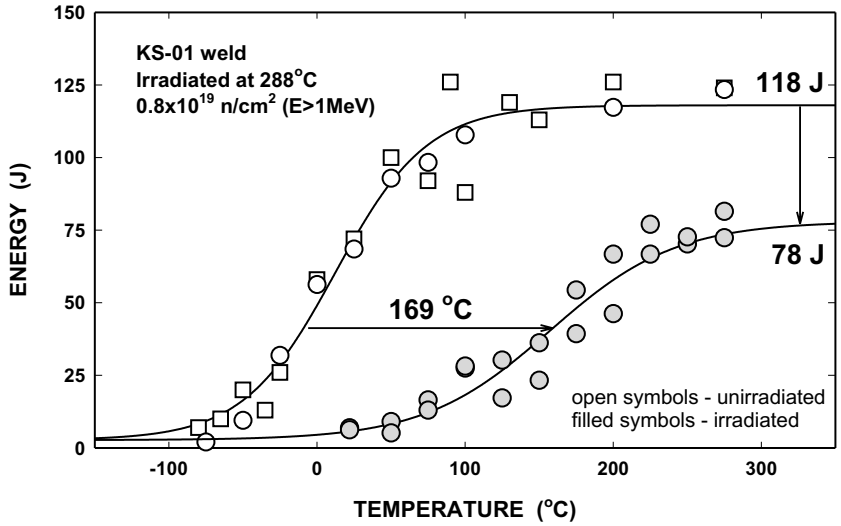

Fig. 2. Temperature dependence of the Charpy absorbed energy of KS-01 weld before and after neutron irradiation.

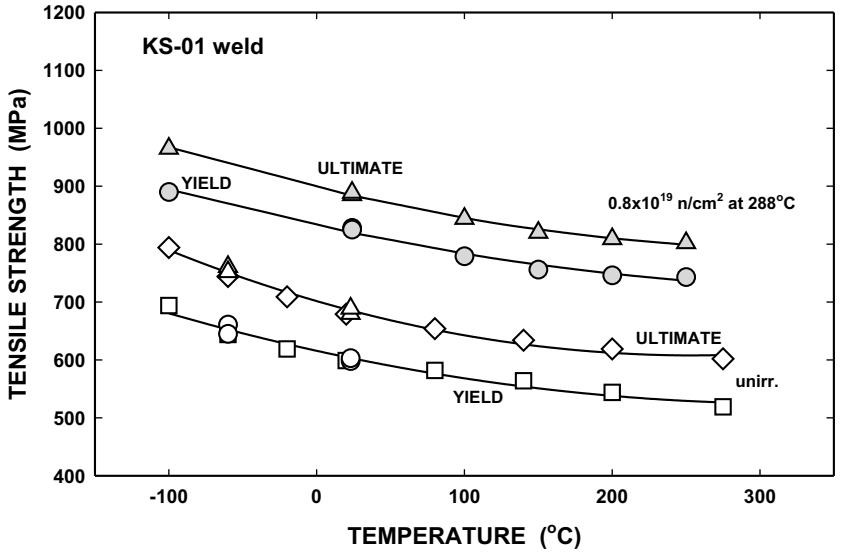

Fig. 3. Temperature dependence of the yield and ultimate strengths of the KS-01 weld before and after neutron irradiation.

determined from positions of the solute atoms in each cluster. A correction was applied to account for the measured variation in the local magnification between the cluster and the matrix. The composition of each

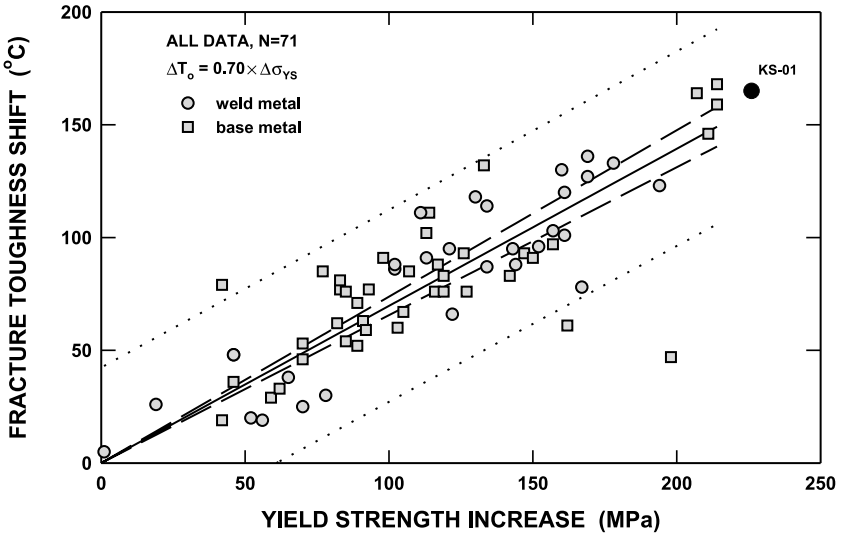

Fig. 4. Relationship between the yield strength increase and the fracture toughness shift for a large RPV database [16] and the position of KS-01 weld data.

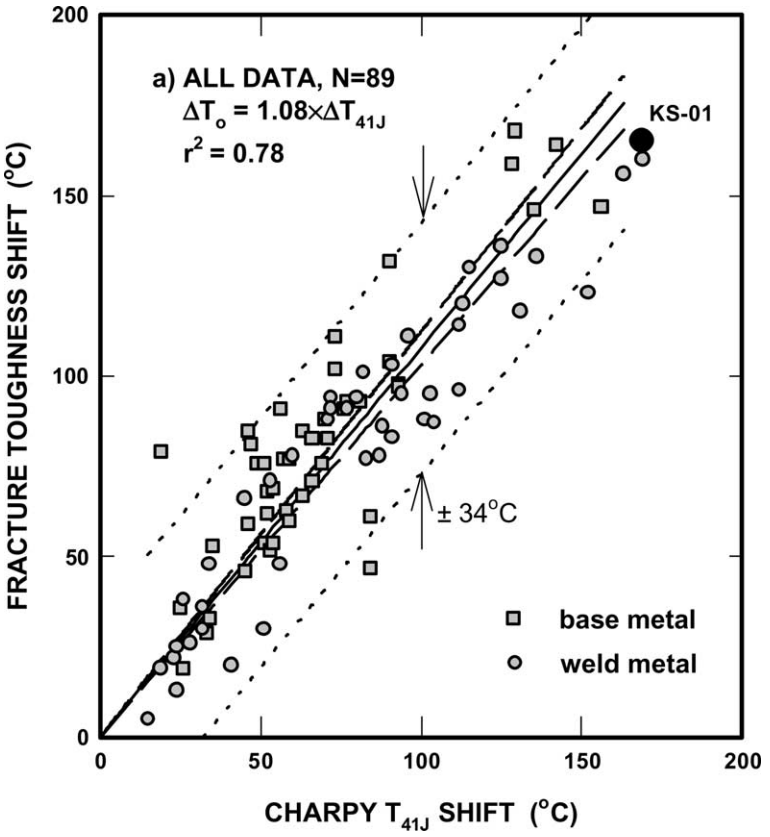

Fig. 5. Relationship between the Charpy T_{41J} and fracture toughness shifts for a large RPV database [16] and the position of KS-01 weld data.

cluster was estimated with the envelope method with a grid spacing of 0.11 nm [1].

3. Results

3.1. Mechanical properties

After neutron irradiation, this weld exhibited a large Charpy T_{41J} shift of 169 K and a significant decrease in upper shelf energy from 118 to ~78 J, as shown in Fig. 2. After neutron irradiation, this weld also exhibited a large shift of the fracture toughness transition temperature of 160 K, as measured by applying the master curve methodology, and an increase in the yield strength from 600 to 826 MPa, as shown in Fig. 3. In addition, the weld exhibited a relatively low ductile initiation toughness (J_{Ic}) after irradiation.

Despite the large shift of the ductile-to-brittle transition temperature and increase in the yield strength, the relationship between embrittlement and hardening of the KS-01 weld follow the general trend for reactor pressure vessel (RPV) steels, as shown in Figs. 4 and 5. The relationship between the yield strength increase and the fracture toughness shift for a large data set of RPV steels [16] and the position of KS-01 weld results relative to this database are shown in Fig. 4. Similarly, a comparison of the Charpy T_{41J} and fracture toughness shifts is shown in Fig. 5. In both cases, the KS-01 weld data are near the upper limit of the data range and follow the general trend within the scatter of data.

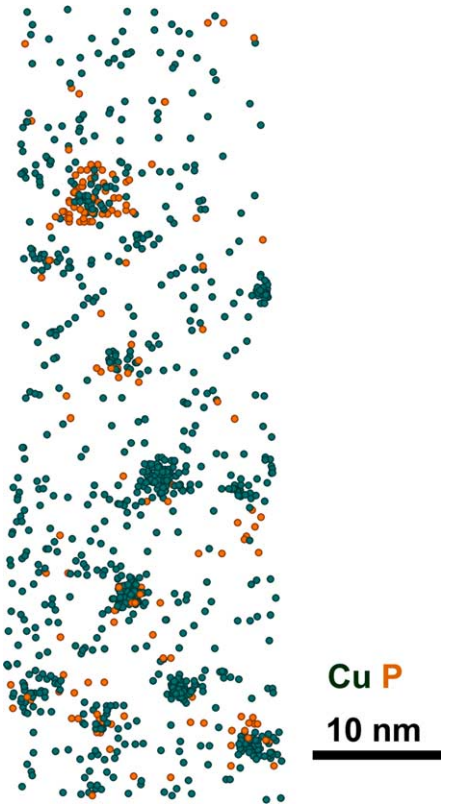

Fig. 7. Atom map of a phosphorus cluster in neutron irradiated KS-01 weld. Phosphorus segregation to the interface of the Cu-enriched precipitates is also evident.

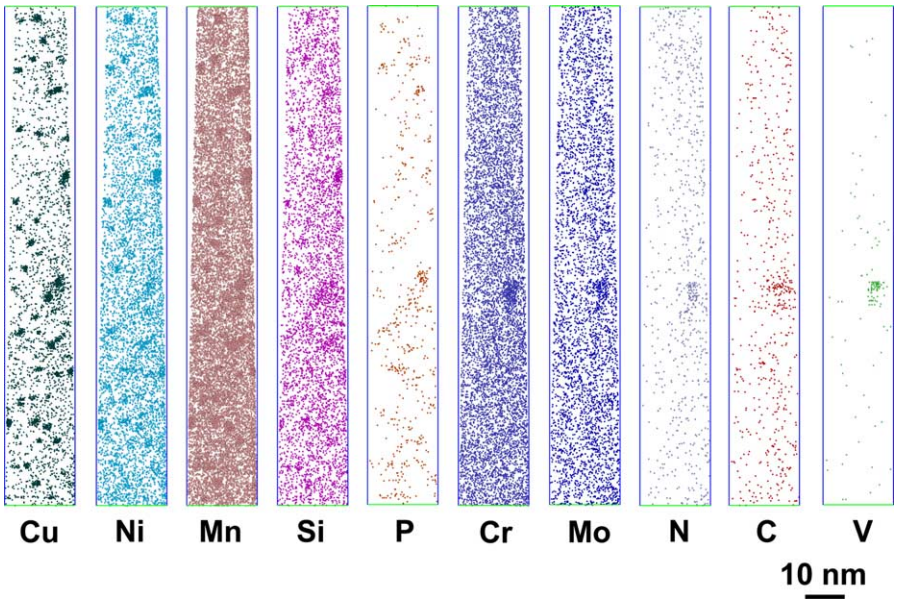

Fig. 6. Atom maps showing the solute distribution in neutron irradiated KS-01 weld. A high number density of Cu-, Mn- Ni-, Si- and P-enriched precipitates is evident. A Cr-, Mn-, Ni-, Cu-, C-, N-, Si- and Mo-enriched feature is also evident.

3.2. Microstructural characterization

Atom probe tomography revealed a high number density ($\sim 3 \times 10^{24}$ m^{-3}) of Cu-, Mn-, Ni-, Si- and P-enriched precipitates in the neutron irradiation weld, as shown in the atom maps in Fig. 6. A lower number density ($\sim 1 \times 10^{23}$ m^{-3}) of roughly spherical and irregularly shaped P clusters was also observed, examples of which are shown in Fig. 7. Some P enrichment was also observed at the interfaces of the Cu-enriched precipitates.

A Cr-, Mn-, Ni-, Cu-, C-, N-, Si- and Mo-enriched feature is also evident in the atom maps shown in Fig. 6. In the N atom map, only the N associated with the MoN^{2+} ions are shown due to the ambiguity of the Si^{2+}/N^{+} at 14 u. A selected volume analysis of this feature yielded a composition of Fe- 5.5 ± 0.7% Cr, 3.7 ± 0.6% Mn, 1.5 ± 0.4% Ni, 1.3 ± 0.4% Cu, 0.7 ± 0.3% C, 0.7 ± 0.3% N, 1 ± 0.3% Si, 1 ± 0.3% V and 1 ± 0.3% Mo. These levels are significantly lower than would be expected for a carbide or nitride precipitate. Therefore, this feature is probably a solute-enriched atmosphere possibly associated with a small dislocation loop. Similar features have been observed by atom probe tomography in neutron irradiated VVER 440 steels [17]. However, the possibility of this feature being a precursor to a carbo-nitride precipitate cannot be excluded.

The ensemble average radius of gyration of the precipitates was determined to be $\langle l_g \rangle = 2.6 \pm 0.5$ nm. The corresponding average element-specific radii of gyration are $\langle l_g^{Cu} \rangle = 2.1 \pm 1.0$ nm, $\langle l_g^{Ni} \rangle = 2.0 \pm 0.9$ nm, and $\langle l_g^{Mn} \rangle = 2.5 \pm 0.5$ nm. Element-specific radii of gyration, l_g^i (i = Cu, Ni, Mn), are plotted as a function of the composite (Cu + Ni + Mn) radius of gyration, l_g, for individual Cu-, Mn-, Ni-, Si- and P-enriched precipitates in Fig. 8. The distribution of points relative to the line of slope = 1 indicates that the Cu and Ni are generally concentrated at the core of the precipitate and the Mn has a more extensive profile into the matrix.

Compositions of individual precipitates were determined by the envelope method [1]. The solute concentrations are plotted as a function of radius of gyration l_g for individual precipitates in Fig. 9. The average composition of these precipitates was Fe- 17.0 ± 9.7 at.% Cu, 31.9 ± 13.8% Ni, 31.7 ± 11.8% Mn, 1.7 ± 1.7% Si, 0.10 ± 0.10% Cr, 0.20 ± 0.2% P, and 0.17 ± 0.17% Mo. The standard deviations, σ, of these concentrations in atomic fraction, c, were determined from the number of individual measurements, m, with the use of the non-biased or '$n-1$' method, i.e., $\sigma = \sqrt{m \sum c^2 - (\sum c)^2 / m(m-1)}$. The large standard deviations are due to significant variations in the solute concentrations, as shown in Fig. 9. The matrix composition is given in Table 1. The standard deviations of the matrix concentrations were estimated from $\sigma = \sqrt{c(1-c)/n}$ where n is the number of atoms in the analysis. The matrix copper level was higher than other atom probe measurement of neutron irradiated pressure vessel steels. However, these lower values were obtained from materials exposed to significantly higher fluences and would indicate that additional copper depletion may occur at higher fluences. These concentration values represent significant enrichments of Cu ($107x$), Ni ($27x$), Mn ($27x$), Si ($5.4x$), and P ($5.9x$), and depletions of Cr ($0.2x$), Mo ($0.6x$) and Fe ($0.2x$) in the precipitates compared to the matrix composition. These results are consistent with the composition of clusters and precipitates in other neutron irradiated pressure vessel steels [3–15].

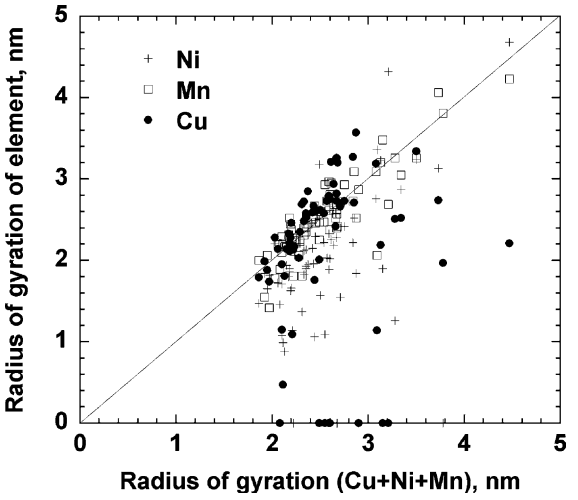

Fig. 8. Element-specific radii of gyration l_g^i (i = Cu, Ni, Mn) plotted vs. the radius of gyration l_g (based on the Cu + Ni + Mn) for individual precipitates.

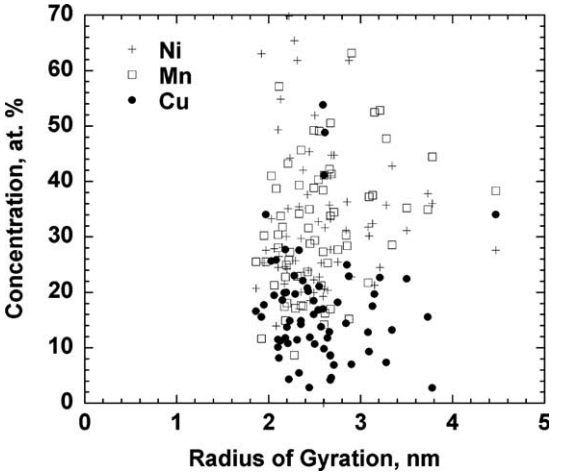

Fig. 9. Concentrations of solute elements versus radius of gyration l_g for individual precipitates as determined by the envelope method.

The size of the P clusters was estimated to be $\langle l_g \rangle = 5.6 \pm 3.3$ nm. The average composition of the P clusters was estimated to be Fe- $54 \pm 12\%$ P, $1.6 \pm 1.6\%$ Mn, $1 \pm 1\%$ Ni, $0.5 \pm 0.5\%$ Cu and $0.5 \pm 0.5\%$ Mo.

4. Conclusions

The atypical KS-01 exhibited more severe embrittlement than other pressure vessel steel welds exposed to similar or higher doses of neutron irradiation. The high copper, manganese and nickel levels in the weld produced a high supersaturation of copper and hence a high number density of copper-, nickel-, manganese-, silicon- and phosphorus-enriched precipitates. The high phosphorus level in the weld also produced a distribution of phosphorus clusters. Although severe embrittlement was observed in the mechanical properties, the data conformed to the master curve.

Acknowledgements

The authors would like to thank Dr R.E. Stoller for his assistance. Research at the Oak Ridge National Laboratory SHaRE Collaborative Research Center was sponsored by the Division of Materials Sciences and Engineering, US Department of Energy, under contract DE-AC05-00OR22725 with UT-Batelle, LLC and by the Office of Nuclear Regulatory Research, US Nuclear Regulatory Commission under inter-agency agreement DOE 1886-N695-3W with the US Department of Energy.

References

[1] M.K. Miller, Atom Probe Tomography: Analysis at the Atomic Level, Kluwer Academic/Plenum Press, New York, NY, 2000.
[2] M.K. Miller, A. Cerezo, M.G. Hetherington, G.D.W. Smith, Atom Probe Field Ion Microscopy, Oxford University, Oxford, UK, 1996.
[3] M.K. Miller, P. Pareige, M.G. Burke, Mater. Charact. 44 (2000) 235.
[4] M.K. Miller, M.G. Hetherington, M.G. Burke, Metall. Trans. A 20 (1989) 2651.
[5] M.K. Miller, P. Pareige, in: G.E. Lucas, L. Snead, M.A. Kirk, R.G. Elliman (Eds.), Proc. MRS 2000 Fall Meeting, Symposium R: Microstructural processes in irradiated materials, Boston, MA, 27–30 November 2000, vol. 650, Materials Research Society, Pittsburgh, PA, 2001, p. R6.1.1.
[6] J.M. Hyde, C.A. English, in: G.E. Lucas, L. Snead, M.A. Kirk, R.G. Elliman (Eds.), Proc. MRS 2000 Fall Meeting, Symposium R: Microstructural Processes in Irradiated Materials, Boston, MA, 27–30 November 2000, vol. 650, Materials Research Society, Pittsburgh, PA, 2001, p. R6.6.1.
[7] M.K. Miller, K.F. Russell, P. Pareige, in: G.E. Lucas, L. Snead, M.A. Kirk, R.G. Elliman (Eds.), Proc. MRS 2000 Fall Meeting , Symposium R: Microstructural Processes in Irradiated Materials, Boston, MA, 27–30 November 2000, vol. 650, Materials Research Society, Pittsburgh, PA, 2001, p. R3.15.1.
[8] M.K. Miller, K.F. Russell, J. Kocik, E. Keilova, J. Nucl. Mater. 282 (2000) 83.
[9] M.K. Miller, K.F. Russell, J. Kocik, E. Keilova, Micron 32 (2001) 749.
[10] M.K. Miller, S.S. Babu, M.A. Sokolov, R.K. Nanstad, S.K. Iskander, Mater. Sci. Eng. A 327 (2002) 76–79.
[11] M.K. Miller, M.A. Sokolov, R.K. Nanstad, S.K. Iskander, Proc. 10th Int. Conf. on Environmental Degradation of Materials in Nuclear Power Systems – Water Reactors, Lake Tahoe, NV, 5–9 August 2001, Pub. NACE, 2002.
[12] M.G. Burke, R.J. Stofanak, J.M. Hyde, C.A. English, W. L. Server, Proc. 10th Int. Conf. on Environmental Degradation of Materials in Nuclear Power Systems – Water Reactors, Lake Tahoe, NV, 5–9 August 2001, Pub. NACE, 2002.
[13] R.G. Carter, N. Soneda, K. Dohi, J.M. Hyde, C.A. English, W. Server, J. Nucl. Mater. 398 (2001) 211.
[14] P. Auger, P. Pareige, S. Welzel, J.C. Van Duysen, J. Nucl. Mater. 280 (2000) 331.
[15] J.M. Hyde, D. Ellis, C.A. English, T.J. Williams, in: S.T. Rosinski, M.L. Grossbeck, T.R. Allen, A.S. Kumar (Eds.), 20th Int. Conf. Effects of Radiation on Materials, ASTM STP 1405, American Society for Testing and Materials, West Conshohocken, PA, 2002.
[16] M.A. Sokolov, R.K. Nanstad, in: Effects of Radiation on Materials: 18th International Symposium, ASTM STP 1325, 1999, p. 167.
[17] M.K. Miller, K.F. Russell, J. Kocik, E. Keilova, J. Nucl. Mater. 282 (2000) 83.